V International Conference on Particle-based Methods – Fundamentals and Applications
PARTICLES 2017
P. Wriggers, M. Bischoff, E. Oñate, D.R.J. Owen, & T. Zohdi (Eds)

NUMERICAL AND EXPERIMENTAL STUDY OF THE POWDER BED CHARACTERISTICS IN THE RECOATED BED OF THE ADDITIVE MANUFACTURING PROCESS

DANIEL S. NASATO[1], MARTIN HEINL[2], TINO HAUSOTTE[2] AND THORSTEN PÖSCHEL[1]

[1]Institute for Multiscale Simulation, Friedrich-Alexander University
Nägelsbachstrasse 49a, 91052 Erlangen, Germany
email: thorsten.poeschel@eam.uni-erlangen.de, web page: www.mss.cbi.fau.de

[2]Institute of Manufacturing Metrology, Friedrich-Alexander University
Nägelsbachstrasse 25, 91052 Erlangen, Germany
email: fmt@fau.de, web page: www.fmt.uni-erlangen.de

Key words: Granular Materials, DEM, Additive Manufacturing, Surface Roughness, Numerical simulation.

Abstract. Part of the optimization steps for additive manufacturing is related to the correct understanding of the mechanical behavior of the powder used in the process. Obtain this understanding based purely on experiments might be a difficult and sometimes prohibitive task. A particle-based numerical tool can provide critical information for correct understanding of powder deposition process. Numerical simulations through the Discrete Element Method (DEM) provide a useful mean to investigate the additive manufacturing process, given the possibility to study particle-scale information that are difficult to access experimentally.

The characteristics of the recoated powder bed are investigated in the packed bed region and onto the manufactured part using PA12 commercial powder. Particle size distribution, contact and non-contact cohesive forces are incorporated in the numerical model. Furthermore, the non-spherical shape of real particles is taken explicitly into account in numerical simulations. A blade-type recoating system is used to form the powder bed and its roughness is calculated.

Experimental measurements are performed by fringe projection. Several areas of the recoated powder layers can be scanned with this optical measurement method. Thus, the analyzed surface roughness can be compared with the simulated quantities to validate the numerical model.

The sintered part is modelled as a prescribed rigid static region in the simulated system. The powder recoated in the sintered region may have different characteristics (packing, roughness) compared to the powder bed region. Recoating process is modelled using two different shapes for the sintered region. The amount of material recoated and the surface roughness are then calculated for the powder bed as well as for the sintered region.

1 INTRODUCTION

Additive manufacturing (AM) is a technique where parts of nearly arbitrarily complex

geometries can be built directly from a three-dimensional (CAD) model by selectively melting layers of powder particles [1]. This has become more and more important for many industrial sectors in the last years and an increasing demand to widen the field of application is noticeable. However, there are still restrictions, e.g. processing speed and product quality, in beam-based additive manufacturing processes like selective laser sintering (SLS) [2].

In particular, understanding the mechanical behavior of the powder particles during the manufacturing process is essential for developing optimization routes towards improved part quality and shorter production time [3].

Discrete Element Method (DEM) describes the trajectory of each individual particle in the system along the time by means of integration of Newton's equation of motion. Useful information to improve part quality and reduce production time can be obtained through numerical simulations using DEM, as particle dynamics are modeled as a function of material properties and particle shape [1,4,5,6]. By choosing the correct collision parameters, particle size and particle shape, the real granular behavior is captured [8,10,11,12].

In this study, a recoating blade is used to spread a layer of particulate PA 12 material over the surface to be sintered. The quality of this layer of powder is investigated through numerical simulations by calculating the surface roughness of the deposited powder in the powder bed and in the sintered region for a recoating speed of 100 mm/s. Experimental measurements of roughness (Rq values) were carried through the fringe projection measuring method after recoating a layer of PA12 polymeric powder and the results were compared to numerical simulations.

The sintered region is of interest and investigated in a limited way. First few layers in the additive manufacturing process are specially affected by the irregular amount of material deposited due to the shrinking of the powder after the melting process. The sintering process is not explicitly simulated in DEM, but its geometry is prescribed using two different shapes. Roughness is calculated in these regions through numerical simulations.

2 METHODOLOGY

2.1. Particle model

Powder deposition process was simulated using the Discrete Element Method (DEM). Real shapes of commercially available PA12 [15] powder were approximated using a clump representation of the particles in the DEM simulations [3,16,17]. In addition, the DEM library LIGGGHTS® [18] was extended to consider bonded and nonbonded attractive particle interaction forces.

Images of commercially available PA12 [15] powder were used as a base to recreate an approximated real particle shape. Sphere are glued together forming a clump of spheres, spatially distributed to capture most of the real shape details. Center of mass and moment of inertia are calculated by means of a Monte Carlo integration, where many points (in the order of 10^6 points) are sampled on an equivalent sphere and points are located inside/outside the composing spheres (contained inside the equivalent sphere), making possible to detect overlapped regions and avoid including these regions twice in the calculations.

To represent the shapes of the sample, 10 different images or real particles [14,15] were used to obtain clumps used in the numerical simulations. Images of the particles and their corresponding DEM model are demonstrated in Figure 1. All templates were equally used

(10% in mass of each template).

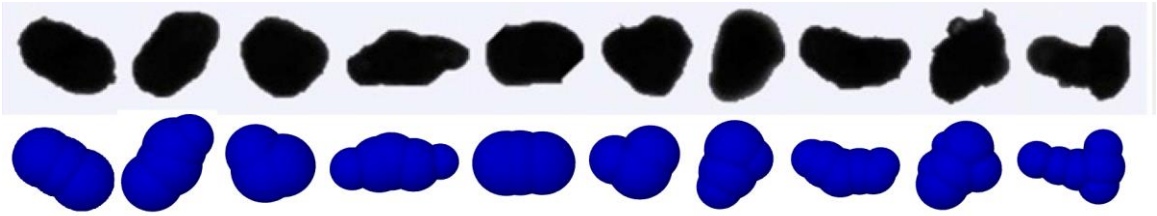

Figure 1 - Images of PA 12 particle templates used in numerical simulations. Top: Images of isolated PA 12 particles obtained through SEM [19]. Bottom: DEM representation of real particles by means of clumps.

Particle size distribution was experimentally measured for PA12 powder in [14]. Based on the experimental cumulative (Q3) distribution 5 different particles sizes were used in the numerical simulations as demonstrated in Figure 2. This size distribution was applied to each of the 10 particle templates shown in Figure 1.

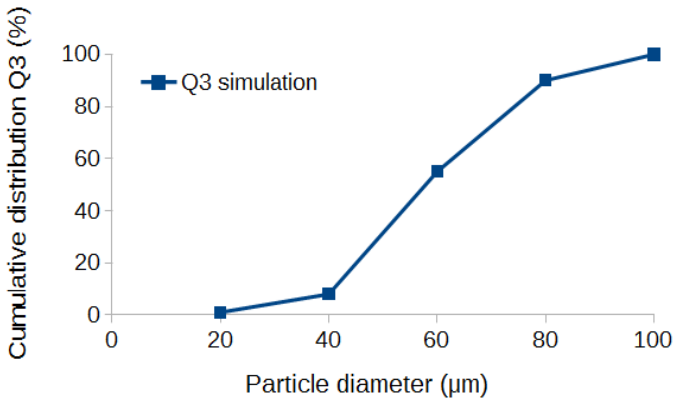

Figure 2- Cumulative distribution (Q3) of particle size adopted in the DEM simulations.

2.2. Inter particle force models

Normal and tangential forces during collision between particles are calculated. A viscoelastic interaction is assumed in the normal direction [20] and a modified Cundall-Strack [21] model is selected for computing the tangential component of the contact force [14]. The normal and tangential terms are given by:

$$\vec{F}_n = min\left(0, -\rho\xi^{\frac{3}{2}} - \frac{3}{2}A_n\rho\sqrt{\xi}\dot{\xi}\right)\vec{e}_n \tag{1}$$

$$\vec{F}_t = -min\left[\begin{array}{c}\mu|\vec{F}_n|, \\ \int_{path}\frac{4G}{2-\nu}\sqrt{R_{eff}\xi}d + A_t\sqrt{R_{eff}\xi}v_t\end{array}\right]\vec{e}_t \tag{2}$$

$$\xi = R_1 + R_2 - |\vec{r}_1 - \vec{r}_2| \tag{3}$$

ξ is the overlap of colliding particles, R_1 and R_2 are the radii of the particles, and $\vec{r}_1$ and $\vec{r}_2$ are their positions. $\vec{e}_n \equiv (\vec{r}_1 - \vec{r}_2)/|\vec{r}_1 - \vec{r}_2|$ is the normal unit vector. The elastic parameter ρ is a function of the effective radius $R_{eff} \equiv R_1 R_2/(R_1 + R_2)$, the Young's modulus Y, and the Poisson's ratio ν, in the form:

$$\rho \equiv \frac{2Y}{3(1-\nu^2)}\sqrt{R_{eff}} \tag{4}$$

The dissipative parameter A_n, depends on the material viscosity [20].

An additional term given by JKR equation is incorporated to the normal viscoelastic model to consider the attractive forces between particles in contact. This term adds an extra normal force in the opposite direction of the elastic force and is given by:

$$\vec{F}_{JKR} = 4\sqrt{\frac{\pi a^3 \gamma Y}{2(1-\nu^2)}}\vec{e}_n \tag{5}$$

where γ is the surface energy density and a is the contact radius related to the overlap in the form:

$$\xi = \frac{a^2}{R_{eff}} - \sqrt{\frac{8(1-\nu^2)\pi a \gamma}{Y}} \tag{6}$$

Due to the relatively small particle size non-contact van der Walls cohesive forces also have a significant influence in the flowability of the particulate material. These forces are incorporated in the DEM model in the following form:

$$\vec{F}_{vdW} = \begin{cases} \left[4\pi\gamma R_{eff}\right]\overrightarrow{e_n}, & if \quad \xi > 0 \\ \dfrac{\left[4\pi\gamma R_{eff}\right]D_{min}^2}{(\xi - D_{min})^2}\overrightarrow{e_n}, & if \quad -D_{max} \le \xi \le 0 \\ 0, & if \quad \xi < -D_{max} \end{cases} \tag{7}$$

where $Dmin = 1.65$ Å is a parameter introduced to avoid the singularity of the Hamaker equation, and $Dmax = 1$ µm is the maximal (cutoff) distance of the van-der-Waals interaction [14]. The intensity of this interaction is characterized by the Hamaker constant A_H, which is given by [14]:

$$A_H = 24\pi D_{min}^2 \gamma \tag{8}$$

The importance of JKR and van der Waals terms in the numerical model was addressed in previous studies when comparing experimental and numerical solid packing fraction [6]. Parameters used for the contact and non-contact force models for PA12 particles in the DEM simulations are depicted in Table 1. Sintered region is fixed - no motion is calculated, but collisions are computed normally.

To validate the inter-particle force model, Ref. [6] compared experimental results for the solid fraction of fine polydisperse powders covering a broad range of particle sizes applied in additive manufacturing. As presented in Ref. [6], predictions from simulations agreed quantitatively very well with the experiments.

Table 1 - Parameters used in contact and cohesion models in the numerical simulations.

Parameter	Symbol	Value
Particle material density	φ	1000 kg/m^3
Young's modulus	Y	2.3x10^7 Pa
Poisson's ratio	ν	0.40
Coulomb's friction coeff.	μ	0.50
Surface energy density	γ	0.1 mJ/m^2
Hamaker constant	A_H	0.2x10^{-21} J

2.3. Recoating process

The simulated system consists of a blade with length of 3 mm. The system has a width (y-direction) of 1mm and periodic boundary conditions are applied in this same direction. The length of the simulation domain is 10 mm (x-direction). The recoating blade was modelled based on the real geometrical characteristics. Only the region which is responsible for the recoating was used to reduce the computational time. Material is initially poured into a reservoir, which is then lifted and the blade spread the particles over the particle bed and the sintered region. The system is demonstrated in Figure 3.

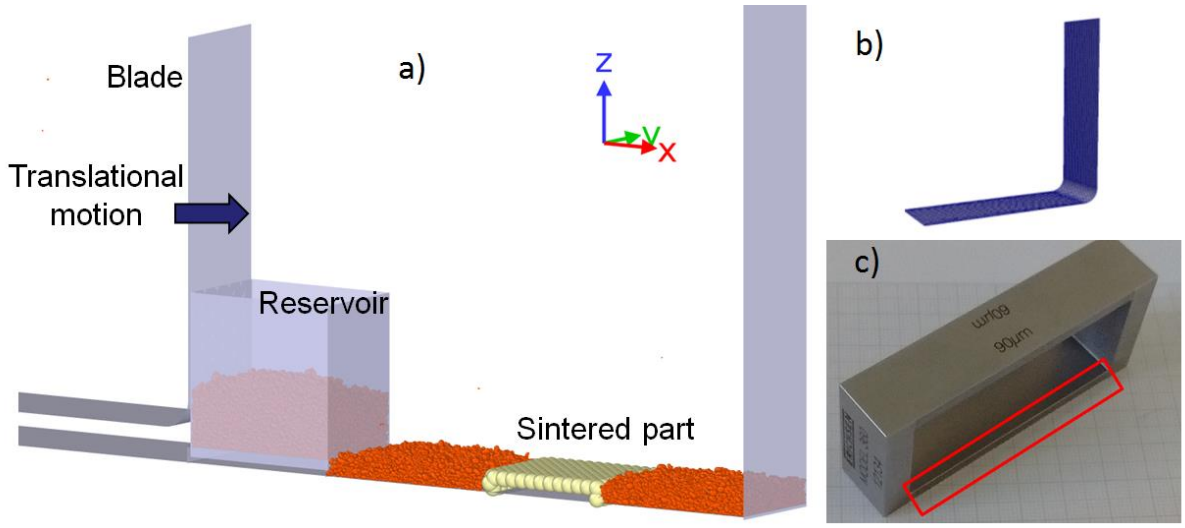

Figure 3 - Simulation domain with indications of the components. a) Translational motion of 100 mm/s is applied to the blade. Particles are recoated over the powder bed and sintered regions. b) details of the recoating blade used in simulations. c) recoating blade used in experiments. In red the region that effectively deposit the layer of material - region modelled in the numerical simulations.

Two different geometries for the sintered part were used, one consisting of a flat shape sintered region, as depicted in Figure 3, and another region of same size but with a concave shape, which can be seen in details in Figure 5.

Roughness was calculated for each of the simulated cases. The mean height of the particles was obtained in the powder bed and in the sintered region and the standard deviation from this mean is the roughness value (Rq) calculated from simulations. This procedure was repeated for three slices in the Y direction to obtain the mean roughness (Rq) and its standard

deviation.

2.4. Experimental procedure

The evaluation of the simulated roughness values has been proved by a surface measurement of several single layers of PA12 powder. The recoating blade dispenses the powder with a thickness of 120 µm and a recoating speed of 100 mm/s. As it is shown in Figure 4 the surface measurement is done by a projection of a planar, periodical and equidistant structured pattern on the recoated layer.

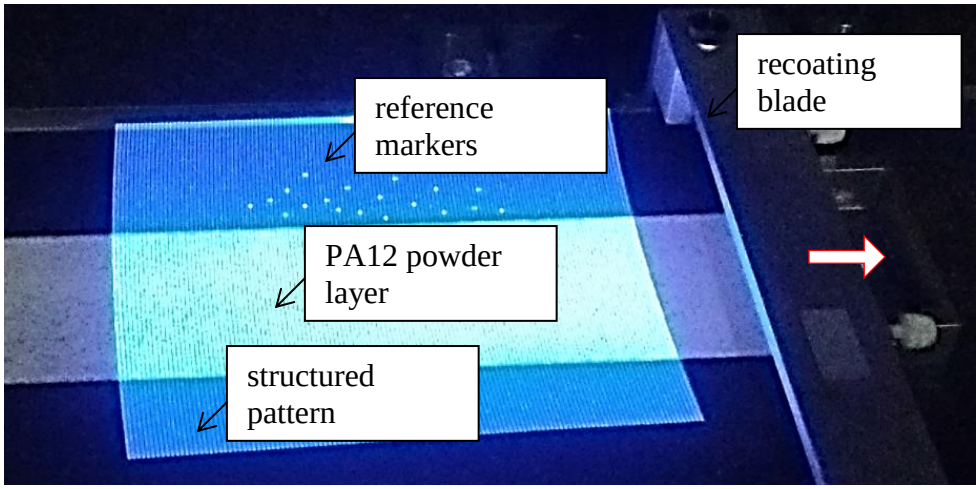

Figure 4 - Surface measurement of the recoated powder by fringe projection

The fringe projection measuring method is implemented by an optical ATOS Compact Scan 2M sensor, which is based on the principle of triangulation. At this point the powder layer is detected with two angled cameras from different observation directions to detect each surface point [22]. In addition, reference points are necessary for the optical observation to match the translational location of the powder in relation to the global coordinate system. The following surface studies are analyzed by TalyMap Platinum software to calculate the profile (2-D-) and the areal (3-D-)roughness parameters.

3 RESULTS

Experimental measurements were performed 3 times and the average values are shown with their respective standard deviation in Table 2. For validation purposes, roughness data calculated through numerical simulations are compared to Rq values. Details of the equations used to obtain the data points are shown in the Appendix.

Numerical results for both flat and concave sintered cases can be seen in Figure 5. A lateral snapshot of both cases is shown for comparison purposes. Differences mainly in the sintered region can be seen and will be quantified in more details. The powder bed region and sintered region considered for the roughness measurements are highlighted.

Table 2 – Experimental measurements of surface roughness and their respective standard deviation (σ). Values are in µm.

	Sa	Ra	Sq	Rq	Sz	Rz
Mean Value	16,00	8,10	20,10	10,20	267,70	45,60
Standard deviation (σ)	4,90	1,80	5,90	2,60	93,30	13,60

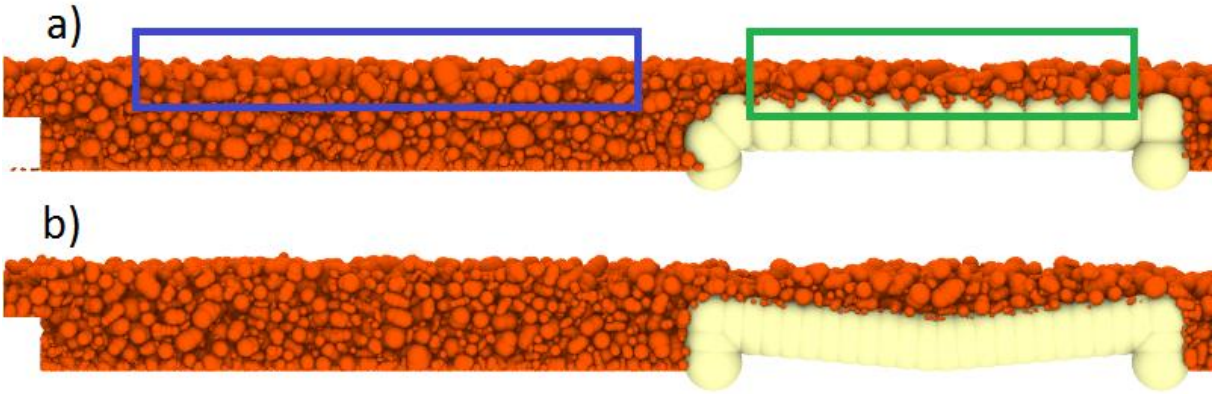

Figure 5 – Recoated powder layer for a) flat sintered region and b) concave sintered region. In blue is the region considered as powder bed region and in green the sintered region used for roughness measurements.

When comparing only the amount of material deposited over the sintered region, an increase of 34% in mass was found from the flat to the concave region (See Figure 6). Such differences in the amount of mass lead to density gradients of the final manufactured part.

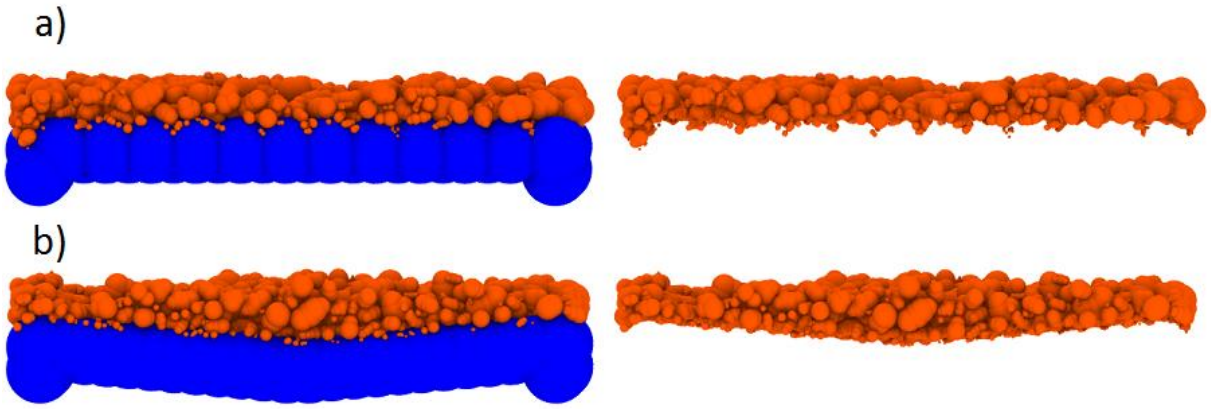

Figure 6 – Details of recoated powder layer for a) flat sintered region and b) concave sintered region. In the right-hand side one can visualize differences in the amount of material deposited for each case.

Surface roughness calculated for both (flat and concave) cases are shown in Table 3. A good agreement between numerical and experimental results was found when comparing the values of the powder bed – deviation of 8.1% for the flat sintered case and 2.7% for the concave sintered case, but still within the standard deviation of the experimental

measurements.

Roughness values for sintered region are relatively higher than those for the powder bed. An increase of 18.7% for the flat shape and 30.9% for the concave shape sintered region compared to their respective bed roughness. This can be attributed to the fact that in the powder bed region particles can penetrate the powder bed and re-accommodate. Also the way forces propagate in a granular or solid region are expected to be different [14]. We also noticed an increase of 16.8% when comparing the roughness of flat with the concave shape sintered.

Table 3 – Numerical results of roughness (Rq) for powder bed and sintered regions and their respective standard deviation (σ). Values are in μm. Results are for flat and concave cases.

Shape	Region	Rq	σ	Rq Experiment	σ
Flat shape sintered	Powder bed	9,37	0,39	10,2	2,6
	Sintered	11,12	1,8		
Concave shape sintered	Powder bed	9,92	0,65		
	Sintered	12,99	1,39		

4 CONCLUSION

A realistic model to simulate the additive manufacturing process using commercially available PA 12 polymeric powder was developed. Bonded and non-bonded cohesive forces were implemented for PA 12 powder, as well as realistic particle shape and particle size distribution. The sintered region was taken explicitly into account in our numerical simulations. Two different shapes for this region were used – one consisting of a flat shape and the other concave shape.

Experimental measurements using fringe projection technique could capture the surface roughness of recoated PA 12. A very good agreement was found from numerical and experimental results when comparing Rq values. Deviations of 8.1% for the flat sintered case and 2.7% for the concave sintered case were found, but still within the standard deviation of the experimental measurements.

The importance of considering the sintered region and its correct shape was also highlighted. Significant increase in roughness (up to 30.9% for concave shape case) was found when comparing to the roughness of the powder bed region. Furthermore, a significant increase (34%) in the mass deposited over the sintered region was also noticed comparing the flat to the concave sintered region. This consolidates the importance of the sintered region, which may lead to gradients in the density of the manufactured part affecting its quality. This is of importance in the initial layers of the manufacturing process, where the differences in the amount of mass recoated in each layer are larger. Sintered region should be explicitly resolved by melting the particles in the recoated layer to obtain a physically correct shape of the sintered region in a more detailed study.

APPENDIX

Table 4 - Definition of roughness parameters.

description	***2-D-roughness parameter (DIN EN ISO 4287)*[23]**	***3-D-roughness parameter (DIN EN ISO 25178-2)* [24]**
arithmetic average roughness	$R_a = \frac{1}{lc}\int \lvert z(x)\rvert dx$	$S_a = \frac{1}{A}\iint \lvert z(x,y)\rvert dxdy$
quadratic average roughness	$R_q = \sqrt{\frac{1}{lc}\int z^2(x)dx}$	$S_q = \sqrt{\frac{1}{A}\iint z^2(x,y)dxdy}$
maximum height roughness	$R_z = z_{max}(x) + z_{min}(x)$	$S_z = z_{max}(x,y) + z_{min}(x,y)$

l_c: measurement length A: measurement surface area $z(x,y)$: height profile

ACKOWLEDGMENTS

The authors want to thank the German Research Foundation (DFG) for funding the Collaborative Research Center 814 (CRC 814) – Additive Manufacturing, sub-projects B1, C4 and B6.

REFERENCES

[1] Campbell, R.I., Bourell, D. and Gibson, I. 2012, 'Additive manufacturing: rapid prototyping comes of age', Rapid Prototyping Journal, 18 (4), pp. 255 – 258.

[2] Schmidt, J., Sachs, M., Blümel, C., Winzer, B., Toni, F., Wirth, K.-E. and Peukert, W. 2014, 'A novel process route for the production of spherical LBM polymer powders with small size and good flowability', Powder Technology 261 pp. 78–86.

[3] Parteli, E.J.R. 2013, 'DEM simulation of particles of complex shapes using the multisphere method: Application for additive manufacturing'. AIP Conf. Proc. 1542, 185; doi: 10.1063/1.4811898.

[4] Zhang, H. P. and Makse, H. A. 2005, 'Jamming transition in emulsions and granular materials'. Phys. Rev. E 72, 011301.

[5] Pöschel, T. and Schwager, T. 2005, Computational Granular Dynamics, Springer, Heidelberg, 322 pp.

[6] Parteli, E.J.R., Schmidt, J., Blümel, C., Wirth, K.-E., Peukert, W. and Pöschel, T. 2014, 'Attractive particle interaction forces and packing density of fine glass powders', Scientific Reports 4: 6227; doi: 10.1038/srep06227.

[7] Zhu, H.P., Zhou, Z.Y., Yang, R.Y. and Yu, A.B. 2007, 'Discrete particle simulation of particulate systems: Theoretical developments', Chemical Enginnering Science 62, pp. 3378-3396.

[8] Paulick, M., Morgeneyer, M. and Kwade, A. 2015, 'Review on the influence of elastic properties on DEM simulation results', Powder Technology 283, pp. 66-76.

[9] Zhu, H.P., Zhou, Z.Y., Yang, R.Y. and Yu, A.B. 2008, 'Discrete particle simulation of particulate systems: A review of major applications and findings'. Chemical Engineering Science 63, pp. 5728-5770.

[10] Alenzi, A., Marinack, M., Higgs, C.F. and McCarthy, J.J. 2013, 'DEM validation using an annular shear cell', Powder Technology 248, pp. 131-142.

[11] Grima, A.P. and Wypych, P.W. 2011, 'Investigation into calibration of discrete element model parameters for scale-up and validation of particle-structure interactions under impact conditions', Powder Technology 212, pp. 198-209.

[12] Bierwisch, C., Kraft, T., Riedel, H. and Moseler, M. 2009, 'Three-simensional discrete element models for the granular statics and dynamics of powders in cavity filling', Journal of the Mechanics and Physics of Solids 57, pp.10-31.

[13] Goodridge, R.D., Tuck, C.J. and Hague, R.J.M. 2012, 'Laser sintering of polyamides and other polymers', Prog. Mater. Sci. 57 pp. 229–267.

[14] Parteli, E.J.R. and Pöschel, T. 2016, 'Particle-based simulation of powder application in additive manufacturing', Powder Technology 288 pp. 96–102.

[15] Rietzel, D., Kühnlein, D., Drummer, D. 2011, 'Selektives Lasersintern von teilkristallinen Thermoplasten', RTejournal Forum Rapid Technol. 6 (urn:nbn:de:0009–2–31138).

[16] Pei, C., Wu, C.-Y. and Adams, M. 2015, 'Numerical analysis of contact electrification of non-spherical particles in a rotating drum', Powder Technology 285 pp. 110-122.

[17] Taghavi, R. 2011, 'Automatic clump generation based on mid-surface', Proceedings of Continuum and Distinct Element Numerical Modeling in Geomechanics, Vol. 1, Melbourne, Australia.

[18] Kloss, C., Goniva, C., Hager, A., Amberger, S. and Pirker, S. 2012, 'Models, algorithms and validation for opensource DEM and CFD-DEM', Prog. Comput. Fluid Dy. 12, pp. 140–152.

[19] Rietzel D, Kühnlein F, Drummer D (2011). Selektives Lasersintern von teilkristallinen Thermoplasten. RTejournal Forum für Rapid Technologie, Vol. 6. (urn:nbn:de:0009231138)

[20] Brilliantov, N. V., Spahn, F., Hertzsch, J.-M. and Pöschel, T. 1996, 'A model for collision in granular gases', Phys. Rev. E 53 pp. 5382–5392.

[21] Cundall, P.A. and Strack, O.D.L. 1979, 'A discrete numerical model for granular assemblies', Geotechnique 29 pp. 47–65.

[22] DIN EN ISO 25178-6: 2010: Geometrical product specification (GPS) – Surface texture: Areal – Part 6: Classification of methods for measuring surface texture parameters. Beuth Verlag, 2010.

[23] CEN - European committee for standardization: DIN EN ISO 4287: 2009-11: 'Geometrical Product Specification (GPS) – Surface texture: Profile method – Terms, definitions and surface texture parameters'.

[24] CEN - European committee for standardization: DIN EN ISO 25178-2: 2012: 'Geometrical product specification (GPS) – Surface texture: Areal – Part 2: Terms, definitions and surface texture parameters'.